Stimulated emission and optical gain in a single MOVPE-grown $Zn_xCd_{1-x}Se$-ZnSe quantum well

R. Tomašiūnas
Institute of Materials Science and Applied Research, Vilnius University, Saulėtekio 10, 2040 Vilnius, Lithuania

I. Pelant
Institute of Physics, Academy of Sciences of the Czech Republic, Cukrovarnicka 10, 162 53 Praha 6, Czech Republic

B. Hönerlage and R. Lévy
1PCMS-GONLO, Unité mixte 380046, CNRS-ULP-EHICS, 23, rue du Loess, 67037 Strasbourg Cedex, France

T. Cloitre and R. L. Aulombard
Groupe d'Etudes des Semiconducteurs, Case Courrier 074, Université de Montpellier II, place Eugene Bataillon, 34095 Montpellier Cedex 05, France

(Received 3 November 1997)

We have studied the stimulated emission from an optically pumped graded index separate confinement heterostructure, realized in the form of a metal-organic vapor-phase-epitaxy-grown single quantum well based on a wide-gap (ZnCd)Se semiconductor. The structure is composed of a central $Zn_{0.78}Cd_{0.22}Se$ quantum well sandwiched between two thicker, zinc-rich (ZnCd)Se layers with a graded cadmium composition varying continuously and monotonously between 0% and 5%. The stimulated emission occurred at ~ 2.49 eV ($T = 8.5$ K), being spectrally redshifted with increasing temperature and disappearing for $T \geqslant 200$ K. The optical gain has been measured using the variable stripe-length method, and values of the gain up to 620 cm^{-1} have been achieved. High-resolution spectral studies of the stimulated emission have revealed a fine structure in the emission spectra originating from different localization sites for excitons. We identify the lasing mechanism as due to an inhomogeneously broadened system of localized excitons. [S0163-1829(98)04320-3]

I. INTRODUCTION

One stage of the search for blue-green semiconductor light emitters was successfully completed some time ago by finding the way how to realize [using molecular-beam epitaxy (MBE)] p doping of the wide-band-gap II-VI semiconductor ZnSe. Structures based on ZnSe have become of increasing technological importance as potential candidates for fabrication of blue-green laser diodes.[1]

Modern semiconductor epitaxy is not restricted to sophisticated MBE, but other methods like the low-cost metal-organic vapor phase epitaxy (MOVPE) are at hand. By MOVPE, however, one meets a difficulty in realizing heavy p doping and, therefore, a p-n junction and laser structures in II-VI materials, despite progress reported recently.[2,3] On the other hand, MOVPE is a suitable method for preparation of graded index separate confinement heterostructures (GRINSCH), in which a single quantum well (QW) is sandwiched between two layers with a monotonously varying energy gap, aimed at better confining of excitons and/or carriers as well as photons in the QW, and at achieving the lowest threshold current for lasing when operated under electrical carrier injection.[4]

In this paper we experimentally study a single $Zn_{0.78}Cd_{0.22}Se$ QW sandwiched between two (Zn,Cd)Se zinc-rich alloy layers with a graded cadmium composition, varying from 0% to 5%. The aim of our investigation is basically twofold. First, to study application-related properties of the QW, like photoluminescence behavior, and the feasibility of obtaining stimulated emission and positive net gain under optical pumping. Second, to contribute to clarifying nature of recombination processes which govern stimulated emission in QW's based on II-VI semiconductors, where various models have been proposed.[5–10] Our preliminary results on the stimulated emission in a MOVPE-grown GRINSCH $Zn_{1-x}Cd_xSe$/ZnSe single QW were published in Ref. 11.

The paper is organized as follows. Section II describes experimental methods and relevant experimental arrangements. Section III deals with the experimental results: transfer of the optical excitation energy into the QW (Sec. III A), properties of the stimulated emission studied with the aid of a variable stripe-length method (Secs. III B and III C) and discussion of extracted optical gain profile (Sec. III D). Section IV is devoted to a discussion of the results.

II. EXPERIMENTAL DETAILS

The sample used in this study was single $Zn_{0.78}Cd_{0.22}Se$ QW of 8-nm thickness grown by low-pressure MOVPE using hydrogen selenide, triethyl-amine-dimethyl zinc, and dimethyl cadmium as precursors. On each side of the QW, layers of (Zn,Cd)Se zinc-rich alloy have been deposited, with a graded cadmium composition continuously and monotonously varying between 0% and 5% of cadmium, the thickness of these being 450 and 350 nm (see Fig. 1). This improves the photon confinement and the efficiency of carrier collection in the QW. A buffer layer of 300 nm of ZnSe

is grown onto a GaAs (100) epitaxy substrate prior the deposition of the $Zn_{0.78}Cd_{0.22}Se$ QW and the cladding layers. Cleaved faces define a cavity length of 600 μm [see Fig. 1(c)].

The investigation of stimulated emission has been performed by using a pulsed XeCl excimer laser (ultraviolet pulses 308 nm with a duration of $\sim$15 ns, at a 5-Hz repetition rate). The laser pulses were focused onto the sample with a cylindrical lens into a stripe of about 20-μm width and of variable length (0–600 μm).[12] The maximum excitation power density on the sample was 300 kW/cm^2. The light emitted by the QW emerged from the cleaved edge of the sample in a direction perpendicular to the exciting beam, it was dispersed by a monochromator and detected by a reticon camera (with the spectral resolution of $\approx$0.05 meV). The measurements were performed in the 8–300-K temperature range, using a continuous helium flow cryostat.

III. EXPERIMENTAL RESULTS

A. Delivery of optical excitation energy into the QW

Pumping pulses of 308 nm, being absorbed strongly in the cap 350-nm-thick layer of (ZnCd)Se, created excitons (e-h pairs) are transported by drift and diffusion into the central QW and recombine there, giving rise to spontaneous and stimulated emissions. The excitons are expected to travel to the QW with a one-dimensional current density

$$j(x) = -D\,\frac{\partial N(x)}{\partial x} + \mu F N(x), \tag{1}$$

where x denotes the direction perpendicular to the surface [Fig. 1(b)], the first term on the right-hand side is due to exciton diffusion, and the second one arises from a driving force $F = -dE_g/dx$ that results from the energy-gap gradient in the cap (Zn,Cd)Se layer. In Eq. (1), D stands for the exciton diffusion coefficient, $N(x)$ denotes the (three-dimensional) exciton concentration, and μ the exciton mobility.

We wish now to estimate the resulting exciton density in the QW. Supposing the validity of the Einstein relation $D = \mu kT$ (kT is the usual Boltzmanns factor) and taking into consideration that $F \approx 0.215$ meV/nm is fixed by the design of our QW,[13] we have to calculate at first the function $N(x)$.

A rate equation governing the process of exciton creation, travel, and recombination in the (Zn,Cd)Se cap layer can be written in the form

$$\frac{\partial N(x,t)}{\partial t} = 0 = \alpha(1-R)Je^{-\alpha x} - \frac{N(x,t)}{\tau} - \mu F\,\frac{\partial N(x,t)}{\partial x} + D\,\frac{\partial^2 N(x,t)}{\partial x^2}, \tag{2}$$

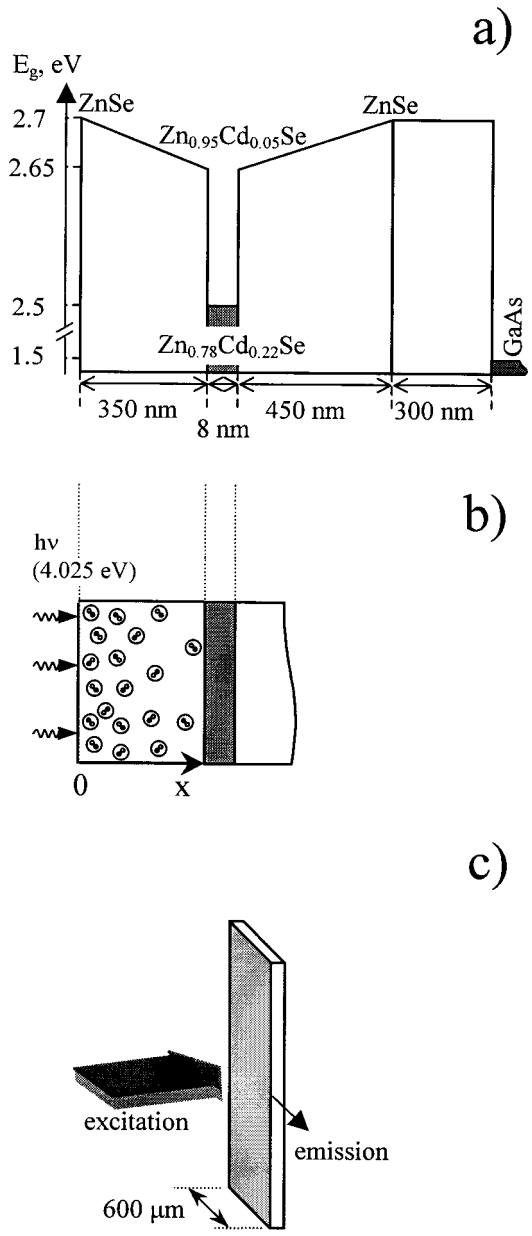

FIG. 1. (a) Schematic sketch of the GRINSCH design. (b) A scheme for the calculation of the exciton transport. (c) The geometry of the experiment to measure the optical gain.

where the first term on the right-hand side describes the optical creation of excitons with the excimer laser of intensity J (α and R stand for the absorption coefficient and reflectivity at 308 nm), the second term is due to exciton recombination (τ is the exciton lifetime) and the last two terms originate from Eq. (1), describing exciton movement from the excited surface to the QW. We consider a stationary case $\partial/\partial t = 0$, because the pump laser pulse duration $\sim$15 ns is much longer than exciton lifetime ($\tau \approx 10^{-10}$ s).[14]

The solution of Eq. (2) is straightforward. We use the boundary conditions $N(x \to \infty) = 0$ and $j(x=0) = 0$. The second boundary condition means that excitons can neither leave the sample nor penetrate into the sample from outside, and it implies $F(x=0) = 0$, $\partial N(x)/\partial x|_{x=0} = 0$. We obtain (for $x > 0$)

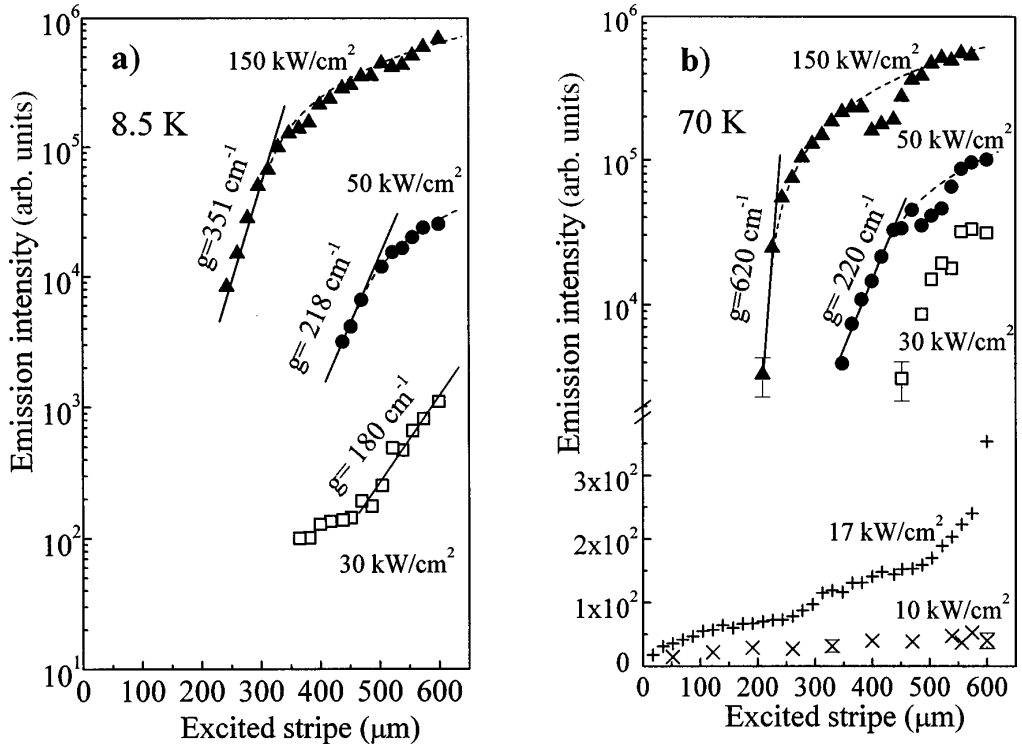

FIG. 2. Emission intensity as a function of the stripe length for the bath temperatures of (a) 8.5 K and (b) 70 K.

$$N(x)=\frac{\alpha(1-R)J}{\frac{1}{\tau}-\alpha^2 D-\frac{\alpha DF}{kT}} \times\left\{\frac{\alpha}{-\frac{F}{2kT}\left[\left(1+\frac{4(kT)^2}{D\tau F^2}\right)^{1/2}-1\right]} \times\exp\left\{-\frac{F}{2kT}\left[\left(1+\frac{4(kT)^2}{D\tau F^2}\right)^{1/2}-1\right]x\right\}+e^{-\alpha x}\right\}. \tag{3}$$

We wish to estimate the upper limit of exciton concentration in the QW before the lasing starts. To this goal we shall consider rather high exciton diffusion constant $D=10\ \mathrm{cm}^2/\mathrm{s}$. In this case Eq. (3) can simplify substantially, since for $F\approx 0.215\times 10^7$ meV/cm, $\alpha\approx 2\times 10^5\ \mathrm{cm}^{-1}$ (Ref. 15), $\tau\approx 10^{-10}$ s (Ref. 14), and $T\leqslant 70$ K the relations $(\alpha^2 D+\alpha DF/kT)\gg\tau^{-1}$ and $4(kT)^2/(D\tau F^2)\ll 1$ hold, and therefore we have (using an approximation $\sqrt{(1+a)}-1\approx a/2$ for $a\ll 1$)

$$N(x)\approx\frac{\alpha(1-R)J\tau}{1+\frac{\alpha kT}{F}}\left(1-\frac{kTx}{D\tau F}\right). \tag{4}$$

Considering that the lifetime of excitons in the QW is equal to that in the cap layer (which is again an upper limit since lifetime shortening is expected for increasing wavefunction overlap of the electrons and holes in the QW), we easily calculate the resulting two-dimensional density σ of excitons in the QW as

$$\sigma=N(d)2a_x, \tag{5}$$

where $d=350$ nm is the distance of the QW from the sample surface and $2a_x=8$ nm is the QW thickness (a_x being the exciton radius). For $T=10$ K, an excitation power density of 150 kW/cm^2 (i.e., $J=2.3\times 10^{23}\ \mathrm{cm}^{-2}\ \mathrm{s}^{-1}$), and a reflectivity $R=0.25$ (Ref. 15), we obtain, with the aid of Eqs. (4) and (5), $\sigma=2.5\times 10^{12}\ \mathrm{cm}^{-2}$. Let us stress that this upper limit of σ is still below the Mott density of similar QW structures [$3\times 10^{12}\ \mathrm{cm}^{-2}$ (Ref. 7) and in $5.1\times 10^{12}\ \mathrm{cm}^{-2}$ (Ref. 6)]. Moreover, the increase in lattice temperature as well as the heating of the exciton gas owing to intense pump pulses [Secs. III B and III D) can lead in the framework of our model [Eq. (3)] only to a decrease of $N(d)$ and, therefore, to a decrease of σ.

It is now of interest to compare relative contributions of the drift $j(x)_{\mathrm{drift}}=\mu FN(x)$ and the diffusion $j(x)_{\mathrm{diff}}=-D\partial N(x)/\partial x$ current densities in Eq. (1). By using Eq. (4), it is easy to obtain a ratio $j(x)_{\mathrm{drift}}/j(x)_{\mathrm{diff}}$ in the form

$$\frac{j(x)_{\mathrm{drift}}}{j(x)_{\mathrm{diff}}}=\frac{D\tau F^2}{(kT)^2}\left(1-\frac{kTx}{D\tau F}\right).$$

For $T=10$ K and the values of the other parameters given above, $j(x)_{\mathrm{drift}}/j(x)_{\mathrm{diff}}\gg 1$. Therefore, it turns out that the drift current (due to the compositional graded cap layer) is much more important than the diffusion current in our experimental conditions.

B. Spectrally integrated stimulated emission from the QW

An unambiguous piece of evidence for the existence of stimulated emission from our sample at low temperatures (8.5 and 70 K) (Ref. 16) is given in Fig. 2, where the emission intensity is displayed as a function of the excited stripe

length. In the variable stripe-length method, part of the spontaneous luminescent radiation with the spontaneous emission rate per unite volume J_{spont} propagates along the stripe axis, and is amplified in the excited region by stimulated emission, and the light intensity at the output J_{stim} is linked with the stripe (excited region) length l by a relation[12]

$$J_{stim}=\frac{J_{spon}A}{g}\,[\exp(gl)-1], \tag{6}$$

where A is the cross-sectional area of the excited volume, and g is the net optical gain (gain due to stimulated emission minus optical loss). Therefore, the exponential variation (for $gl \gg 1$) of the light output with increasing l, shown in Fig. 2 by full lines, proves the existence of stimulated emission, and from the slope of J_{stim} (on log scale) against l the values of the optical gain can be easily extracted. Let us note that the onset of the stimulated emission could easily be checked with the naked eye: an extremely bright blue-green spot suddenly appeared at the facet of the sample.

For large l, saturation of the emission intensity in Fig. 2 can be clearly seen. Such a saturation is due to exhaustion of excited radiative centers and leads to only linear variation of the light output with stripe length for long enough stripes (see the dashed lines in Fig. 2). However, noticeable deviations from these linear variations in the form of ''notches'' can be recognized, especially at $T_{bath}=70$ K [Fig. 2(b)]. The origin of these deviations is probably linked with the spectral composition of the amplified emission. We will come back to this point below. Another interesting feature in Fig. 2 is that the optical gain at 70 K is higher than at 8.5 K.

C. Spectrally resolved stimulated emission

Figure 3 displays the emission spectra taken at $T_{bath}=70$ K under 17-kW/cm^2 excitation intensity for various excited stripe lengths. The threshold of the stimulated emission, characterized by a sudden narrowing of the emission line, can be clearly seen. It is worth mentioning that the spectra given in Fig. 3 correspond to the last few points (the longest stripe lengths) on the curve denoted 17 kW/cm^2 in Fig. 2(b), where the starting superlinear increase of the emission intensity indicates just the onset of the positive net gain.

It is important to note that the stimulated emission arises directly within the spontaneous simple spectral line profile peaked at 2.486 eV, i.e., there is no indication of any new emission line appearing with increasing stripe length, which could represent the opening of a radiative channel.

What is the origin of the spontaneous emission band? Low-temperature wavelength derivative reflectivity measurements have revealed that the lowest exciton structure in a $Zn_{0.78}Cd_{0.22}Se/ZnSe$ quantum well is located at about 2.52 eV.[17] Therefore, the spontaneous (as well as stimulated) emission occurs in the low-energy tail of the $n=1$ heavy-hole (HH) exciton resonance. Both observations described above (the onset of the stimulated emission directly from the spontaneous line profile and the spectral location of the stimulated emission on the low-energy wing of the $n=1$ HH exciton resonance) bear a close resemblance to the results of Ding and co-workers,[5,6] who prescribed the light emission and lasing in $Zn_{1-x}Cd_xSe/ZnSe$ quantum wells to a system of excitons localized in the well due to alloy compositional

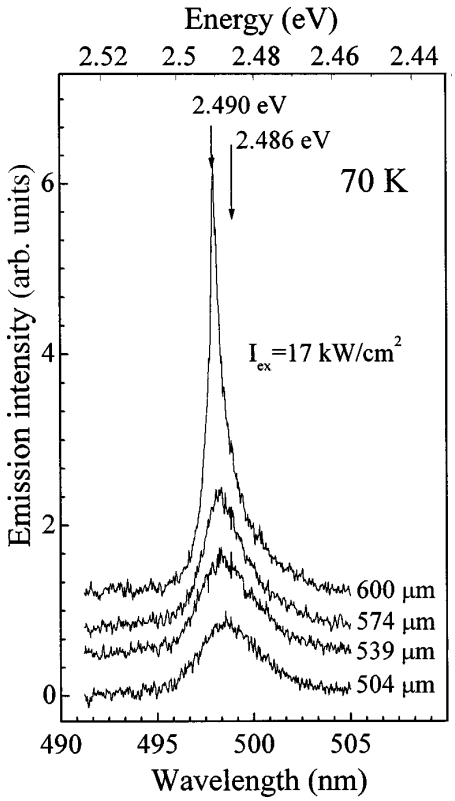

FIG. 3. Evolution of the emission spectrum with increasing stripe length ($T_{bath}=70$ K, excitation intensity 17 kW/cm^2).

fluctuations and random well thickness variations. The reason for exciton persistence in II-VI QW systems is that, unlike III-V semiconductors, the binding energy of quasi-2D excitons can exceed the LO-phonon energy,[6,17] thus avoiding exciton dissociation and stabilizing the exciton system against electron-hole plasma formation. Such a system causes inhomogeneous broadening of the exciton line shape as a result of a Gaussian-like energy distribution of localized exciton states. Once photocreated, excitons begin to occupy preferentially the deepest local band-gap minima (thus resembling a Fermi-like system), and their recombination radiation is expected to occur in the low-energy tail of the absorption and/or reflection resonance.

Indeed, the lack of a ''doublet structure'' in our spontaneous as well as stimulated emission spectra strongly disqualifies the free excitonic molecule as well as the free exciton-exciton scattering and the free-exciton–LO-phonon scattering mechanisms from participating in optical gain formation in our case, because all of them are characterized by a separate spectral feature well below the exciton resonance.[18] In addition, we have observed virtually no redshift of the stimulated emission by increasing the excitation intensity even by an order of magnitude.[11] This eliminates in addition the mechanism of the electron-hole plasma radiative recombination.

We performed a detailed high-resolution study of the stimulated emission. An example is given in Fig. 4, which displays variations of the spectral shape with the stripe-length at $T_{bath}=70$ K and $T_{bath}=8.5$ K. A fine structure, modulated upon a wider background [$\leqslant 10$ meV full width at half maximum (FWHM)], can be clearly recognized.

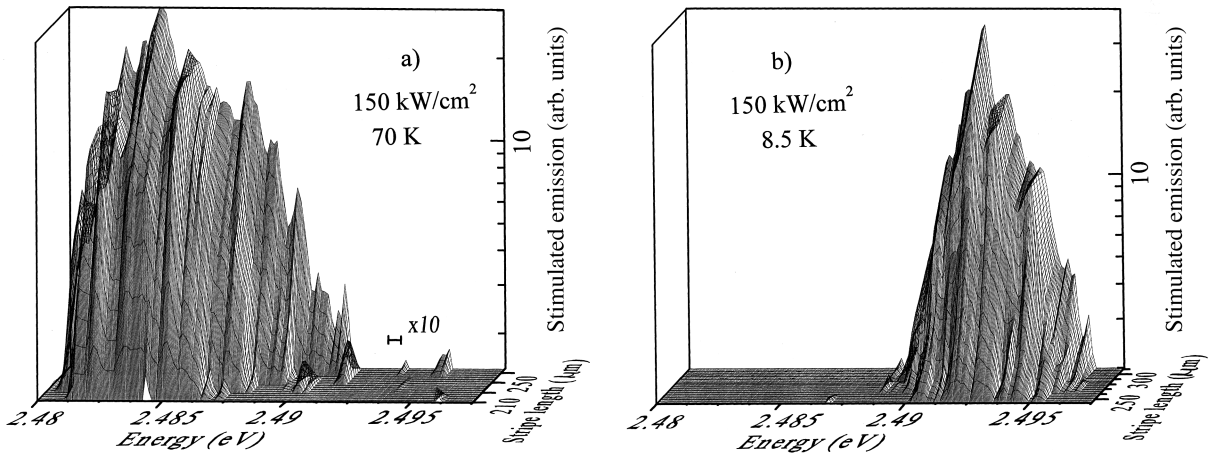

FIG. 4. Stimulated emission spectra vs the stripe length, taken under the pump intensity of 150 kW/cm^2: (a) bath temperature 70 K, (b) bath temperature 8.5 K.

What is the origin of this fine structure? We can certainly eliminate cavity modes because (i) far from the full length of the sample (only 250 μm from 600 μm) was photoexcited, and (ii) the fine structure develops in a somewhat irregular way by increasing the stripe length. Rather, we believe that the fine structure represents individual homogeneously broadened contributions of the localized excitons: The irregularities in the spectral structure development reflect a (spatially) irregular distribution of excitonic traps.

Direct support to this interpretation can be obtained by comparing Figs. 2 and 5. In particular, the ''dips'' on the curves displayed in Fig. 2(b) are very likely germane to distinct modifications in the spectral profile of the stimulated emission, as demonstrated in Fig. 5. For instance, the deviation from the expected linear variation—dashed line—in Fig. 2(b), occurring at 50 kW/cm^2 for stripe lengths $\geqslant$450 μm, seems to be correlated with ''switching over'' the peak photon energy from $h\nu_1 \approx 2.489$ eV to $h\nu_2 \approx 2.487$ eV [see Fig. 5(a)]. We prescribe this observation to a terraced variation in the QW thickness by several atomic layers at a given site x_0: Let us suppose that the gain on photon energy $h\nu_1$ attains its equilibrium value for stripe lengths $l > x_0$ in the ''narrower'' part of the QW, then saturates, and the light output increases henceforth only linearly with increasing l. For high enough $l = l_0 (> x_0)$ the reabsorption of the low-energy wing of the stimulated emission at $h\nu_1$, that happens in the ''wider'' part of the QW ($l < x_0$) and contributes to its photopumping, results in attainment of population inversion in this QW part, and photons leaving the sample facet have energy $h\nu_2 < h\nu_1$.

The entire process manifests itself as a discontinuity (dip) at a given value of the stripe length l_0 on the curve emission intensity vs stripe length, due to the gain onset at $h\nu_2$ and its fast saturation ($l_0 \approx 450\ \mu$m for a pump intensity of 50 kW/cm^2). It is intuitively clear that such a dip will shift to higher values of l_0 with decreasing laser pump power density, and this is exactly what can be seen in Figs. 2(b) and 5.

Let us now discuss the effect of temperature on the emission spectra. Evolution of the stimulated emission spectrum with temperature variation is displayed in Fig. 6(a). The peak photon energy undergoes a redshift (principally due to the band-gap shift), and lasing is gradually weakened and disappears for $T_{\text{bath}} \geqslant 200$ K. The decrease in intensity with increasing temperature is accompanied with a line-shape broadening. A remarkable feature of the spectra (that can also be noticed in Fig. 5) is that their low-energy sides are smooth while the high-energy sides are distinctly structured.

All these attributes, shown in more detail in Fig. 6(b), could perhaps be plausibly explained again in terms of lasing due to inhomogeneously broadened localized exciton resonance: The localized excitons fill up the low-energy wing of the Gaussian absorption profile. The increase in homogeneous linewidth of the individual components with temperature[6] results in their stronger overlapping and enhanced reabsorption, as shown schematically in inset of Fig. 6(b). Predominantly high-energy photons undergo the reabsorption (because higher excited states are less occupied), in this way causing an evident ''cutting out'' of the high-energy side of the spectrum, and an accentuation of its structure. In the high-temperature limit this leads finally to homogeneous line broadening, when the lasing system passes over from a three-energy-level to a two-energy-level scheme (exciton states from which the gain is possible plus the ground state).[19] It is well known that in a two-level excitonic system lasing cannot be achieved without the participation of a third particle,[20] and this is consistent with our observation: Stimulated emission vanishes at $T_{\text{bath}} \geqslant 200$ K, and the homogeneous broadening due to exciton–LO-phonon interaction, becomes a prevailing factor beyond $T \geqslant 200$ K as shown in Sec. III D.

D. Gain profile

The spectral profile of the optical gain $g(E)$ is one of the principal characteristics of a lasing medium. We extract an experimental $g(E)$ in the usual way from two emission spectra $I_{\text{stim1}}(E)$, $I_{\text{stim2}}(E)$, measured for two different stripe lengths l_1 and l_2, with the aid of the relation

$$\frac{I_{\text{stim1}}(E)}{I_{\text{stim2}}(E)} = \frac{\exp[g(E)l_1] - 1}{\exp[g(E)l_2] - 1}, \tag{7}$$

that follows immediately from Eq. (6). Care has been taken to take values l_1 and l_2 from the nonsaturated region. An

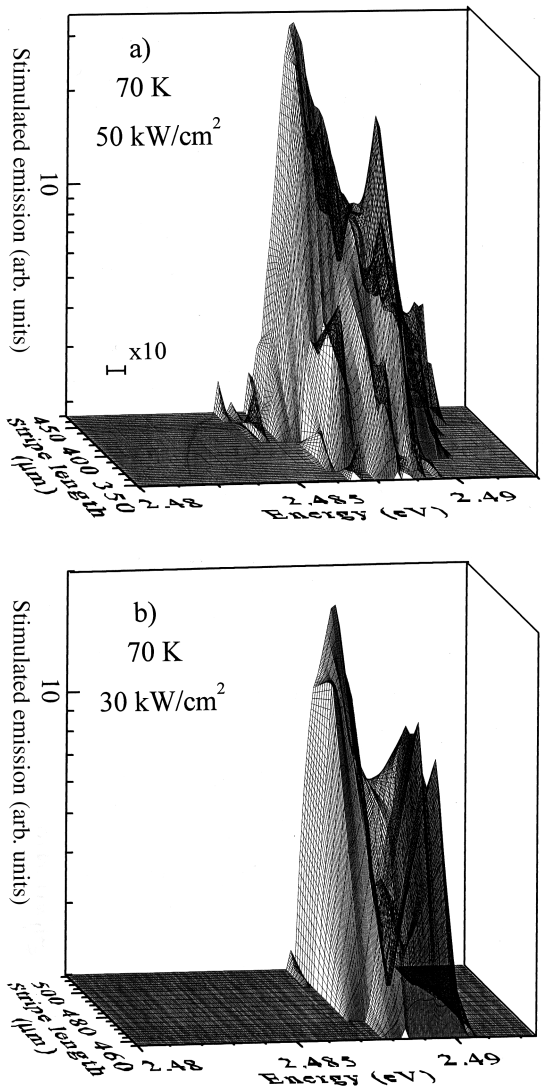

FIG. 5. Stimulated emission spectra vs the stripe length, taken at a bath temperature of 70 K for (a) a pump intensity of 50 kW/cm^2, and (b) a pump intensity of 30 kW/cm^2.

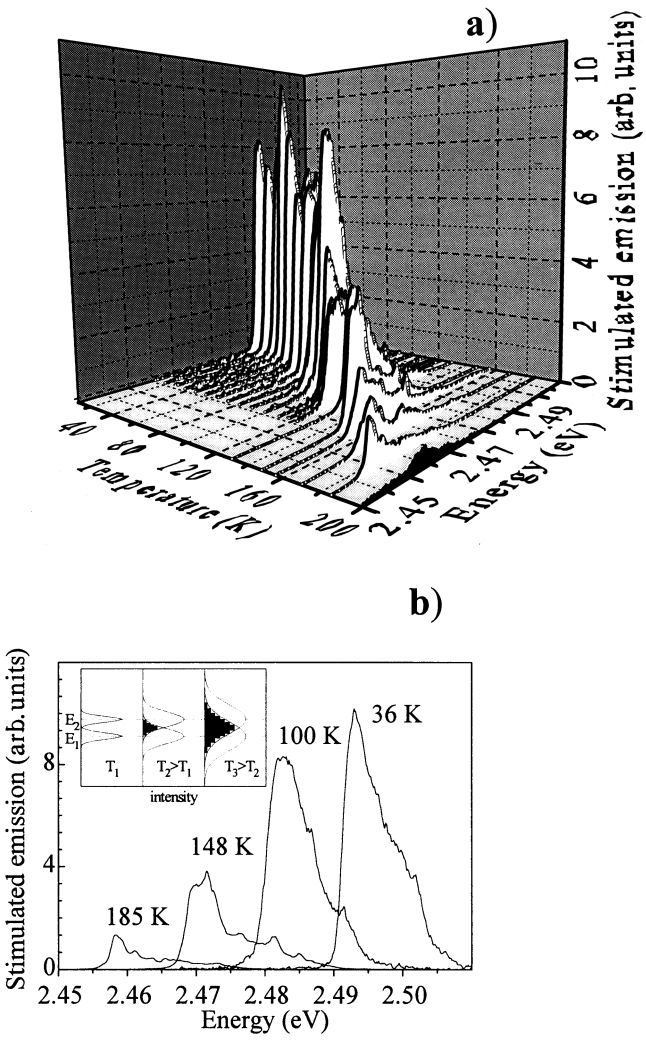

FIG. 6. (a) Overall view on the evolution of the stimulated emission spectra as a function of the bath temperature. The pump intensity is 300 kW/cm^2. The anchored line of the spectra at 200 K is the spontaneous lujminescence mujltiplied by 10. (b) Selected stimulated emission spectra from (a). The inset schematically shows the increase in homogeneous linewidth with increasing bath temperature, which leads to a quenching of the stimulated emission; see text.

example demonstrating the evolution of $g(E)$ when going from 30 to 150 kW/cm^2 at $T_{\text{bath}}=70$ K is shown in Fig. 7 (points). To compare this experimental result with a theoretical gain profile, we make use of the relation[6]

$$g(E)=D_i(E)[2\,f(E)-1]=D_i(E)\left[\frac{2}{e^{(E-\mu)/kT_{\text{eff}}}+1}-1\right], \tag{8}$$

that holds in the limit of an extreme inhomogeneous broadening, and describes a ''Fermi-like'' system of localized excitons occupying successively higher and higher excited states within the Gaussian[21] inhomogeneous line-shape profile $D_i(E)$. In Eq. (8), $f(E)$ denotes the Fermi distribution function, μ is the chemical potential, and T_{eff} is an effective temperature of the exciton system.

To calculate $g(E)$ on the basis of Eq. (8), values of T_{eff} and of the Fermi level μ, and the function $D_i(E)$ have to be known. Since in our case we excite highly above the band gap, we have to consider that the excitons thermalize, giving rise to a moderate lattice heating, also, more importantly, due to the short exciton lifetime the distribution of localized excitons is described by an effective exciton temperature $T_{\text{eff}}>T$ (lattice temperature). The effective temperature can be found from fitting the high-energy wing of the spontaneous emission spectrum, which is described by a Boltzmann distribution $\sim e^{-h\upsilon/kT_{\text{eff}}}$. In this way we obtain T_{eff}(150 kW/cm^2)=210 K, T_{eff}(50 kW/cm^2)=180 K, T_{eff}(30 kW/cm^2)=160 K, and T_{eff}(17 kW/cm^2)=140 K [see an example for 17 kW/cm^2 case in the inset in Fig. 7(a)].

We take the general distribution function of the localized excitons $D(E)$ as a normalized Gaussian profile, with the FWHM given as

$$\Gamma=\Gamma_0+\frac{\Gamma_{\text{LO}}}{e^{\hbar\omega_{\text{LO}}/kT}-1}, \tag{9}$$

where $\Gamma_{\text{LO}}=36$ meV (Ref. 6) and $\hbar\omega_{\text{LO}}=31.3$ meV (Ref. 17). We shall show shortly that $D(E)\approx D_i(E)$ under our

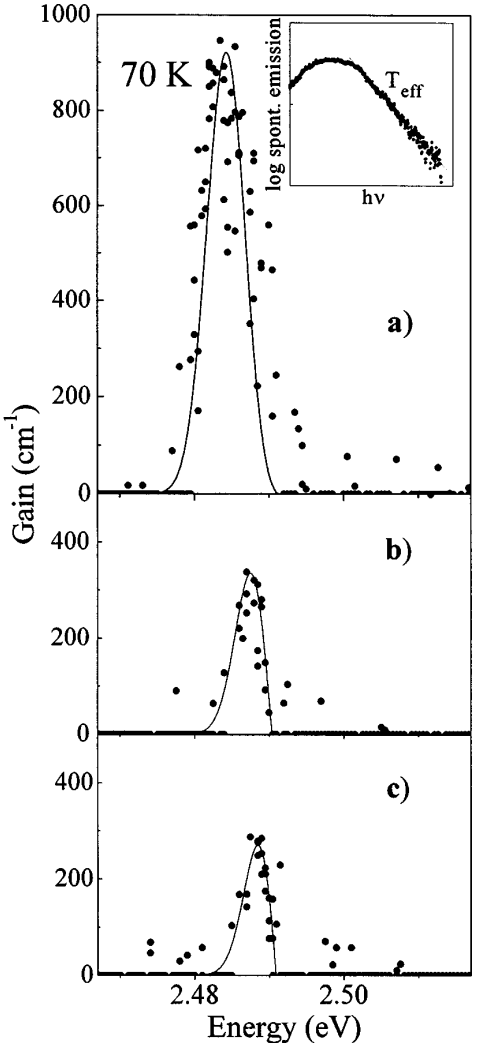

FIG. 7. Experimental (points) and theoretical (full lines) gain profiles. The theoretical curves have been calculated according to Eq. (8). For parameters of the calculation, see text. The experimental data have been measured under pump intensities of (a) 150 kW/cm^2, (b) 50 kW/cm^2, and (c) 30 kW/cm^2. The bath temperature $T_{bath}=70$ K. The inset demonstrates the extraction of the effective temperature T_{eff} of the exciton gas from the spontaneous emission line shape.

experimental conditions. The remaining two variable parameters to calculate $g(E)$ are thus Γ_0 (the inhomogeneous broadening) and μ. The experimentally observed relatively narrow widths of the gain curves (Fig. 7) act as a strongly limiting factor for the choice of Γ_0. We then arrive at the best theoretical modeling of the experimental gain curves (see the full lines in Fig. 7) by fixing $\Gamma_0=6$ meV and taking the following values of μ with respect to the center of the distribution function $D(E)$: $\mu(30\ \text{kW/cm}^2)=-0.3899$ meV, $\mu(50\ \text{kW/cm}^2)=0.50037$ meV, and $\mu(150\ \text{kW/cm}^2)=5.8297$ meV. Let us note that the filling factor of the distribution function $D(E)$ in the case of 150-kW/cm^2 pumping intensity equals ≈ 0.58, i.e., we fill up approximately one-half of the sites available for exciton localization.

Good agreement between the experiment (points) and the calculated gain curves (full lines) can be seen in Fig. 7. Two items have to be clarified here. First, there is clearly a redshift of the gain curves with increasing pump intensity, although increasing filling up of the Gaussian profile should lead rather to a blueshift. We attribute this redshift to the lattice heating mentioned above. For 150 kW/cm^2, the shift amounts to about 6 meV, and corresponds to an increase in the *lattice* temperature T by about ≈ 12 K (from a bath temperature from 70 K to ~ 82 K), as inferred from the temperature dependence of the fundamental gap in $Zn_{1-x}Cd_xSe$ alloys.[22] To achieve a final good fit to experimental gain profiles, the calculated curves were shifted horizontally on the energy axis according to the actual spectral positions of the experimental ones.

Second, the values of the FWHM calculated with the aid of Eq. (9) (taking into consideration even the minor lattice heating) amount to $\leqslant 6.5$ meV. This means that the site distribution function $D(E)$ is basically still governed by inhomogeneous broadening ($\Gamma_0=6$ meV), i.e., $D(E)\approx D_i(E)$, and we have a right to use Eq. (8) to evaluate $g(E)$. At the same time, it follows from Eq. (9) that for $T\geqslant 200$ K the parameter Γ (FWHM) attains values $\geqslant 13\ \text{meV} > 2\Gamma_0$, and the homogeneous broadening thus becomes a prevailing factor.

IV. DISCUSSION

The single $Zn_{0.78}Cd_{0.22}Se/ZnSe$ GRINSCH QW studied in the present work exhibits stimulated emission with relatively very high optical gain (up to $\sim 600\ \text{cm}^{-1}$ at $T_{bath}=70$ K), much the same or even higher in comparison with multiple ZnSe/CdSe QW structures,[6,7,14,23] although it is somewhat difficult to make a direct comparison because of different experimental conditions. We explain the origin of the gain as due to an inhomogeneously broadened system of localized excitons. The localization occurs in local potential minima arising as a result of compositional disorder and variations in the QW thickness. In Sec. III, we enumerated the main experimental observations leading to the above-mentioned interpretation:

(i) There is no indication of any new emission line below exciton resonance linked with the onset of the stimulated emission. The stimulated emission emerges from the low-energy wing of the spontaneous emission line (Fig. 3).

(ii) Stimulated emission spectra are characterized by noticeable irregular fine structure, representing individual homogeneously broadened contributions of the localization sites (Fig. 4).

(iii) Behavior of the stimulated emission as a function of the temperature (Fig. 6): the increasing weight of homogeneous broadening with increasing temperature leads (along with obvious luminescence thermal quenching) to a loss of lasing.

It is worth mentioning that the widening of the gain profile with increasing photoinjection (Fig. 7) is also in full conformity with the scenario of higher filling of the inhomogeneous Gaussian distribution (or shift of the chemical potential μ to higher energies). Of course, we observe qualitatively the same picture for free-carrier plasma lasing (i.e., increase in the gain width with increasing photoinjection). In the case of a two-dimensional plasma, however, the plasma chemical potential should vary linearly with the photoinjection level,[24] and this would imply a much more pronounced increase in gain width than that shown in Fig. 7. On the other

hand, the redshift in gain (in Fig. 7) could seemingly indicate gap shrinkage due to the plasma occurrence, but free-carrier plasma emission is expected to be found here on the *high-energy* side of the exciton resonance, due to exciton localization. The redshift just mentioned arises therefore as a consequence of the sample heating. This lattice heating is due to fast thermalization of hot excitons via LO-phonon emission. The elevated lattice temperature is to be distinguished from the effective temperature (T_{eff}) describing the distribution of localized excitons. Another argument against dominant free-carrier plasma participation in a lasing mechanism is the presence of the fine structure on the high-energy wing of the stimulated emission, even under the highest photoinjection level of 300 kW/cm^2 (Fig. 6).

These results are in qualitative agreement with recent observations on exciton localization in $Zn_{1-x}Cd_xSe/ZnSe$ multiple QW: In high-x samples with relatively deep wells ($x \approx 0.2-0.3$, i.e., including our QW with $x=0.22$), exciton localization manifests itself in photoluminescence dynamics, while in shallow wells with low x ($x \approx 0.1$) the density of localization centers N_D is low, their occupation is rapidly saturated, and exciton screening and an electron-hole plasma formation follow.[9,25] However, we find no quantitative agreement concerning the magnitude of localization center density: N_D was found to be 4×10^{10} cm^{-2} for $x=0.23$ in Ref. 9, but in the present work we observe no saturation up to $\sim10^{12}$-cm^{-2} exciton concentration.

Another puzzling point at first sight is the fact that we observe a lower net gain at 8.5 K than at 70 K (see Fig. 2). Because of the temperature increase which causes ''washing out'' of the Fermi distribution $f(E)$ in the vicinity of the Fermi level, an expected trivial consequence is less effective overlapping of $D_i(E)$ with $\{2f(E)-1\}$ in Eq. (8) and, consequently, a lower gain at higher temperatures. This has not been observed; however, it was shown in Ref. 26 that the transfer rate of excitons into the QW increases with temperature, and at sufficiently high temperatures is overcome by recombination through nonradiative channels. This may result, together with temperature variations of waveguide properties of the GRINSCH structure, in a maximum on the gain curve vs temperature. The steeper ''edge'' of the Fermi distribution in the vicinity of the Fermi level at lower temperatures may then account for the fact that there is a modest high-energy side spreading of the stimulated emission spectra in Fig. 4(b) ($T_{\text{bath}}=8.5$ K) and, conversely, a more gradual Fermi distribution edge at higher temperatures may allow the high-energy side of the spectrum to spread considerably, as observed in Fig. 4(a) ($T_{\text{bath}}=70$ K).

Finally, we wish to mention that quite recently Mikulskas *et al.*[27] studied a complete series of single MOVPE-grown $Zn_{1-x}Cd_xSe/ZnSe$ GRINSCH quantum wells from the point of view of the optical gain, by applying the same experimental approach as that used throughout this paper. On the plot of stimulated emission intensity vs stripe length (analogous to Fig. 2 in the present work) they observed two gain regions. The first gain appears at relatively small stripe lengths (0–100 μm), and reaches saturation very soon. The second gain mechanism starts at considerably longer stripe lengths ($l_s>400$ μm). The values of the optical gain are lower in the region of the second gain; nevertheless the relevant emission intensities are higher. The authors explain these observations by invoking two different gain mechanisms: (i) exciton immediate localization in the localized states with a Gaussian distribution (the first gain), and (ii) exciton-exciton inelastic scattering that is resonantly enhanced due to the presence of the localized states (the second gain).

A question arises as to whether we are able to identify our gain measurements with the first or second gain mechanism mentioned above. To answer this question, we wish to point out that the results of Ref. 27 show a clear tendency to minimize the differences between the first and second gain regions (it means shifting the second gain region toward the first gain region) with increasing gain values, i.e., with increasing quality of the sample. It can be expected that the both gain regions ''merge'' together in the limit of samples of high enough gains, i.e., the second gain mechanism no longer appears. The gain values measured in the present work are comparable with those of the samples in Ref. 27, which implies that the GRINSCH structure used in the present work is of the same quality as the series of samples in Ref. 27. Therefore, in our case the gain mechanism can be clearly identified (except the case of very low pump intensities) with the so-called first gain, whose mechanism in fact we invoke to interpret our results throughout the paper.

V. SUMMARY AND CONCLUSIONS

In summary, we have presented a detailed study of the stimulated emission and optical gain in the (ZnCd)Se/ZnSe GRINSCH single QW. Although very intense stimulated emission has been observed at low temperatures (mainly in the range 8–100 K), a rapid decrease of the lasing has been observed for $T_{\text{bath}}\geqslant150$ K, and no stimulated emission has occurred above 200 K. Further improvement in the architecture and/or composition of the GRINSCH systems is therefore indispensable to comply with demands for the realization of laser diodes operating at room temperature. Concerning the mechanism which rules the laser action, our results point, in accord with other reports,[5,6,14,25] to the important role of the excitonic system in II–VI QW's.

In particular, we have observed a fine structure in the stimulated emission spectra that we interpret as a manifestation of individual (homogeneously broadened) contributions of localized excitons. This represents direct evidence of involvement of localized excitons in the optical gain formation in (ZnCd)Se/ZnSe QW systems.

ACKNOWLEDGMENTS

Two of us (R.T. and I.P.) thank the French Ministry of Education and Scientific Research for financial support (Contract Nos. 132650C and 1353/AP/MDLM/CB, respectively). This work has been partially supported by the Commission of the European Communities under an ESPRIT III Basic Research Contract No. 6675-MTVLE. We thank D. Brinkmann for valuable discussions.

[1] See, e.g., M. A. Haase, J. Qiu, J. M. DePuydt, and H. Cheng, Appl. Phys. Lett. **59**, 1272 (1991).
[2] H. Stanzl, K. Wolf, B. Hahn, and W. Gebhart, J. Cryst. Growth **145**, 918 (1994).
[3] K. Ogata, T. Kera, D. Kawaguchi, Sz. Fujita, and Sg. Fujita, J. Cryst. Growth **170**, 507 (1997).
[4] C. Weisbuch and B. Vinter, *Quantum Semiconductor Structures* (Academic, New York, 1991).
[5] J. Ding, H. Jeon, T. Ishihara, M. Hagerott, A. V. Nurmikko, H. Luo, N. Samarth, and J. Furdyna, Phys. Rev. Lett. **69**, 1707 (1992).
[6] J. Ding, M. Hagerott, T. Ishihara, H. Jeon, and A. V. Nurmikko, Phys. Rev. B **47**, 10 528 (1993).
[7] F. Kreller, M. Lowisch, J. Puls, and F. Henneberger, Phys. Rev. Lett. **75**, 2420 (1995).
[8] L. Canganile, D. Greco, P. V. Giugno, R. Rinaldi, P. Prete, R. Cingolani, A. Franciosi, L. Sorba, and L. Vanzetti, Solid State Commun. **97**, 713 (1996).
[9] M. Lomascolo, M. Di Dio, D. Greco, L. Canganile, R. Cingolani, L. Vanzetti, L. Sorba, and A. Franciosi, Appl. Phys. Lett. **69**, 1145 (1996).
[10] R. A. Taylor, R. A. Adams, J. F. Ryan, and R. M. Park, J. Cryst. Growth **159**, 822 (1996).
[11] R. Tomasiunas, I. Pelant, D. Guennani, J. B. Grun, R. Lévy, O. Briot, B. Gil, R. L. Aulombard, and J. M. Sallèse, Solid State Commun. **97**, 187 (1996).
[12] K. L. Shaklee and R. F. Leheny, Appl. Phys. Lett. **18**, 475 (1971).
[13] We make use of the compositional dependence law of the band gap of the unstrained alloy in the form $E_g(\mathrm{Zn}_{1-x}\mathrm{Cd}_x\mathrm{Se}) = 2820 - 1530x + 510x^2$ (Ref. 16), which for $\Delta E_g = E_g(\mathrm{ZnSe}) - E_g(\mathrm{Zn}_{0.95}\mathrm{Cd}_{0.05}\mathrm{Se})$ and $d = 350$ nm, yields $dE_g/dx \approx \Delta E_g/d \approx 0.125$ meV/nm$\approx 3.14\times10^{-14}$ J/m.
[14] J. Gutowski, A. Diessel, U. Neukirch, D. Weckendrup, T. Behr, B. Jobst, and D. Hommel, Phys. Status Solidi B **187**, 423 (1995).
[15] S. Adachi and T. Taguchi, Phys. Rev. B **43**, 9569 (1991).
[16] It should be stressed that we operate with three different temperatures in the paper: (i) T_{bath} describes the temperature of the cooling medium (He gas). (ii) T means the temperature of the crystalline lattice in the QW, and slightly exceeds T_{bath} owing to the thermalization of the exciton gas. (iii) T_{eff} denotes the effective temperature of the exciton system in the QW. It holds that $T_{\mathrm{bath}} < T < T_{\mathrm{eff}}$.
[17] F. Liaci, P. Bigenwald, O. Briot, B. Gill, N. Briot, T. Cloitre, and R. Aulombard, Phys. Rev. B **51**, 4699 (1995).
[18] C. Klingshirn and H. Haug, Phys. Rep. **70**, 315 (1981).
[19] We apply nonresonant optical pumping via free-electron-hole pair creation highly above the gap in the cap layer; nevertheless, it is not a three-energy-level scheme because of the very fast energy relaxation and transfer to localized exciton states in comparison with the quasistationary situation in the QW, as discussed in Sec. III A.
[20] *Excitons at High Density*, edited by H. Haken and S. Nikitine, Springer Tracts in Modern Physics Vol. 73 (Springer, Berlin, 1975).
[21] F. Yang, G. R. Hayes, R. T. Phillips, and K. P. O'Donnel, Phys. Rev. B **53**, R1697 (1996).
[22] L. Malikova, W. Krystek, F. H. Pollack, N. Dai, A. Cavus, and M. C. Tamargo, Phys. Rev. B **54**, 1819 (1996).
[23] R. Cingolani, R. Rinaldi, L. Calcagnile, P. Prete, P. Sciacovelli, L. Tapfer, L. Vanzetti, G. Mula, F. Bassani, L. Sorba, and A. Franciosi, Phys. Rev. B **49**, 16 769 (1994).
[24] R. Cingolani and K. Ploog, Adv. Phys. **40**, 535 (1991).
[25] R. Cingolani, L. Canganile, G. Colí, R. Rinaldi, M. Lomoscolo, M. DiDio, A. Franciosi, L. Vanzetti, G. C. LaRocca, and D. Campi, J. Opt. Soc. Am. B **13**, 1268 (1996).
[26] L. Aigouy, J. P. Alexis, O. Briot, T. Cloitre, B. Gill, R. L. Aulombard, and M. Averous, Superlatt. Microstruc. **17**, 381 (1995).
[27] I. Mikulskas, K. Luterova, R. Tomasiunas, B. Hönerlage, T. Cloitre, and R. L. Aulombard (unpublished).